JPn Neuroscience
The Journal of Physiology

J Physiol 590.22 (2012) pp 5597–5610

Mammalian prestin is a weak Cl^-/HCO_3^- electrogenic antiporter

P. Mistrík[1], N. Daudet[1], K. Morandell[1] and J. F. Ashmore[1,2]

[1] *UCL Ear Institute, 332 Gray's Inn Road, London WC1E 6BT, UK*
[2] *Department of Neuroscience, Physiology and Pharmacology, UCL, Gower Street, London WC1E 6BT, UK*

Key points

- Outer hair cells of the mammalian cochlea are cells which amplify the incoming sound using mechanisms based on prestin, a molecular actuator related to a family of chloride–bicarbonate exchangers.
- It has not been clear so far whether prestin has any bicarbonate–chloride exchange properties, often being described as an 'incomplete transporter'.
- Here we show, using a pH probe linked to prestin in an expression system, that prestin can transport bicarbonate at low rates and acts as an electrogenic transporter for chloride.
- The high expression level of prestin in mammalian outer hair cells thus accounts for a number of previous observations of the cells' internal pH regulation, and may indicate an additional role for prestin in homeostatic regulation of cochlear amplification.

Abstract The lateral membrane of mammalian cochlear outer hair cells contains prestin, a protein which can act as a fast voltage-driven actuator responsible for electromotility and enhanced sensitivity to sound. The protein belongs to the SLC26 family of transporters whose members are characterised as able to exchange halides for SO_4^{2-} or HCO_3^- yet previous analyses of mammalian prestin have suggested that such exchange functions were minimal. Here anion transport is investigated both in guinea-pig outer hair cells (OHCs) and in an expression system where we employ a sensitive intracellular pH (pH_i) probe, pHluorin, to report HCO_3^- transport and to monitor the small pH_i changes observable in the cells. In the presence of extracellular HCO_3^-, pH_i recovered from an acid load 4 times faster in prestin-transfected cells. The acceleration required a chloride gradient established by reducing extracellular chloride to 2 mM. Similar results were also shown using BCECF as an alternative pH_i sensor, but with recovery only found in those cells expressing prestin. Simultaneous electrophysiological recording of the transfected cells during bicarbonate exposure produced a shift in the reversal potential to more negative potentials, consistent with electrogenic transport. These data therefore suggest that prestin can act as a weak Cl^-/HCO_3^- antiporter and it is proposed that, in addition to participating in wide band cochlear sound amplification, prestin may also be involved in the slow time scale (>10 s) phenomena where changes in cell stiffness and internal pressure have been implicated. The results show the importance of considering the effects of the endogenous bicarbonate buffering system in evaluating the function of prestin in cochlear outer hair cells.

(Resubmitted 23 July 2012; accepted after revision 10 August 2012; first published online 21 August 2012)
Corresponding author J. F. Ashmore: Department of Neuroscience, Physiology and Pharmacology, UCL, Gower Street, London WC1E 6BT, UK. Email: j.ashmore@ucl.ac.uk

Abbreviations GFP, green fluorescence protein; LJP, liquid junction potential; OHC, outer hair cell.

DOI: 10.1113/jphysiol.2012.241448

Introduction

Prestin is a membrane protein expressed at high levels in the lateral membrane of cochlear outer hair cells (OHCs) of the mammalian inner ear (reviewed in Ashmore, 2008; Dallos, 2008). Identified in 2000 (Zheng *et al.* 2000), prestin's properties provide an explanation for OHC voltage-dependent length changes first observed over two decades ago (Brownell *et al.* 1985; Kachar *et al.* 1986; Ashmore, 1987). The properties of prestin also determine the mechanism responsible for mammalian sound amplification, for prestin's conformational changes are intrinsically fast (Frank *et al.* 1999) and recent reports suggest that the OHC time constant may not limit its response bandwidth *in vivo* (Johnson *et al.* 2011), a problem previously thought to limit prestin's role in high-frequency cochlear amplification. There are various models for prestin's molecular mode of action, but the predominant view is that the conformational changes of the molecule depend on partial transmembrane movements of chloride ions (Oliver *et al.* 2001).

Prestin is the fifth member of the SLC26 superfamily of transporters involved in epithelial ion exchange (for review see Dorwart *et al.* 2008). This family contains SO_4^{2-} transporters, halide/HCO_3^- exchangers and some members which are reported to exhibit Cl^- channel-like properties. However, in the case of mammalian prestin, SLC26A5, no significant unidirectional transport has been detected when monovalent (HCO_3^-, Cl^-) or divalent (SO_4^{2-}) anions were tested (Oliver *et al.* 2001; Schaechinger & Oliver, 2007). Instead, monovalent anions (Cl^-, HCO_3^-) have been proposed as forming the extrinsic voltage sensor in these proteins when they act as 'incomplete' transporters, so that movement of these anions from the intracellular surface triggers changes in molecular conformation. Antiporter models, incorporating partial transfer of anions across the membrane, can be developed to give reasonable agreement with experimental data (Muallem & Ashmore, 2006). Nevertheless, radioactive-uptake studies challenge the model of prestin as an incomplete transporter as it can be shown that prestin is able to transport both monovalent (formate, thiocynate) and divalent (oxalate) anions although not necessarily those implicated in normal physiological processes (Rybalchenko & Santos-Sacchi, 2008; Bai *et al.* 2009; Schanzler & Fahlke, 2012).

As with other members of the SLC26 family, prestins from some species exhibit non-neutral transport. In particular, rat prestin is able to transport SCN^- electrogenically (Schanzler & Fahlke, 2012). By creating recombinant prestins it has been shown that regions of the prestin amino acid sequence are implicated in transport and motility (Schaechinger *et al.* 2011; Tang *et al.* 2011), but as yet, short of a tertiary structure for prestin, the relationship between electromotility and transport remains unclear.

In order to investigate the transporting properties of mammalian prestin further and in situations closer to the physiological state of the molecule, in particular to determine whether it is indeed able to act as a Cl^-/HCO_3^- antiporter, we developed a novel strategy to monitor changes in intracellular pH (pH_i) induced by transport of HCO_3^-. Bicarbonate is found at physiological levels in cochlear fluids and would seem to be the main cerebrospinal fluid buffer (Wangemann, 2006). We first demonstrated that outer hair cells show responses compatible with a Cl^-/HCO_3^- antiport behaviour as suggested originally by Ikeda and coworkers (Ikeda *et al.* 1992). To simplify the system further, however, we used an expression system with an intracellular pH sensor, choosing Superecliptic pHluorin (Miesenbock *et al.* 1998). This genetically modified green fluorescence protein (GFP) has significantly increased pH sensitivity compared with the native protein. Therefore, when fused with prestin using DNA recombinant techniques, pHluorin permits (1) an identification of successfully transfected cells and (2) measurements of intracellular pH in a close spatial proximity to a prestin molecule. As a control, pHluorin was tagged with the myristylation-targeting peptide to facilitate intracellular anchoring in the cellular membrane (Cross *et al.* 1984). A direct comparison of fluorescence from cells transfected with either prestin–pHluorin or pHluorin thus provides an efficient and sensitive way to identify prestin-dependent pH changes.

As well as showing transport both by conventional pH sensing experiments and by electrophysiological measurements in OHCs, the imaging experiments in the expression system below show that prestin can transport HCO_3^- in a manner dependent on the chloride gradient across the cell membrane. In combination with patch-clamp measurements, the exchange is consistent with an electrogenic exchange, exhibiting a shift in reversal potential compatible with a stoichiometry of 2 HCO_3^-:1 Cl^-.

Methods

Cloning of the pMb–pHluorin and pBK–CMV–rprestin–pHluorin constructs

The plasmid containing the cDNA of rat prestin was a gift from B. Fakler (Freiburg). Plasmids containing the pHluorin coding sequence (Miesenbock *et al.* 1998) were obtained from J. Henley (Bristol) and G. Miesenbock (Oxford). To generate the membrane-targeted pHluorin construct (pMb–pHluorin), the coding sequence of pHluorin was PCR-amplified with modified primers containing BamH1 (5′ end of pHluorin) and Not1 (3′ end of pHluorin) sites and cloned into PCR-BluntII

TOPO vector (Invitrogen). The BamH1/Not1 pHluorin fragment was then inserted in frame and downstream of a v-src myristoylation sequence (MGSSKSKPKDPSQRR), into a BamH1/Not1 digested CMV-containing plasmid for eukaryotic gene expression (derived from pEGFP-N1, Clontech).

A pBK-CMV plasmid driving expression of a rat prestin–GFP fusion protein (pBK–CMV–rprestin–GFP) was used as a backbone for generating the prestin–pHluorin expression construct (pBK–CMV–rprestin–pHluorin). First, a modified PCR-based overlap extension method (Wurch *et al.* 1998) was used to clone into PCR-BluntII TOPO a DNA fragment consisting of the 5′ end of rat prestin (from nucleotide 1557/BST1107I restriction site in the rat prestin sequence) fused in frame with the pHluorin coding sequence (containing a HindIII site at the 3′ end). The pBK–CMV–rprestin–GFP was then digested with BST1107I and HindIII to replace its original (BST1107I-3′ end of rprestin–GFP–HindIII) fragment with the (BST1107I-3′ end rprestin–pHluorin–HindIII) fragment previously generated by overlap extension PCR.

All PCR reactions were performed using a high-fidelity DNA polymerase (Phusion, New England Biolabs) and the identity of the plasmids was confirmed by sequencing.

Outer hair cell measurements

Outer hair cells from the apical turns 3 and 4 of the guinea-pig cochlea were used in the experiments to be reported. All animal handling and tissue preparation was carried out in accordance with UK Home Office regulations. Briefly, adult guinea-pigs (250–350 gm) were killed by rapid cervical dislocation and the bullas removed for further dissection in standard extracellular solution given below. For the imaging experiments using BCECF as the pH_i indicator, isolated cells were prepared for viewing on an inverted microscope as described previously (Géleoc *et al.* 1999). Cells were selected that were lightly stuck down onto the surface of the chamber on an inverted microscope and therefore stable against solution change. For electrophysiological experiments involving solution changes over prolonged periods, small strips 2–4 mm in length of apical cochlea were dissected out and placed gently in the experimental chamber on an upright microscope (Olympus BX51, with a 60× 1.0 NA WI objective), allowing solution changing while permitting access to the basal poles of the OHCs with the recording pipette. The tissue was held in place by using gold-plated electron microscopy grids (50 mesh, Agar Scientific, UK) to prevent movement during the perfusion. The added stability and minimised mechanical damage during dissection was found to permit stable recordings from single cells that could be maintained regularly for at least 20 min.

Expression cell culture and heterologous expression

Chinese hamster ovary (CHO)-K1 cells were grown in F-12 Ham medium supplemented with 10% fetal bovine serum (FBS, Invitrogen), 200 mM L-glutamine, 100 U ml^{-1} penicillin and 100 $\mu g\ ml^{-1}$ streptomycin, and incubated at 37°C with 10% CO_2. The prestin-related DNA constructs were delivered into CHO-K1 cells using lipofectamine reagent (Invitrogen). For the experiments measuring non-linear capacitance, HEK293 cells were used instead but grown under identical culture conditions.

Solutions

Standard extracellar solutions were (in mM): NaCl, 140; $CaCl_2$, 1; $MgSO_4$, 1; KCl, 4; Hepes, pH 7.4, with glucose added to 320 mOsmol l^{-1}. In solutions where bicarbonate was used, the Hepes buffer was replaced with 25 mM sodium bicarbonate, equilibrated with 5% CO_2 to maintain pH and NaCl reduced to 115 mM to maintain osmolarity. In extracellular solutions with low Cl^- concentrations (1–6 mM), chloride was replaced with gluconate. For ammonium-containing solutions, 50 mM NH_4Cl replaced NaCl. The pH was adjusted to 7.4 with NaOH and the osmolarity kept at 320 mOsmol l^{-1} with glucose. Solutions were changed by a local exchange system, which replaced the solution in the bath within 60 s. All chemicals were purchased from Sigma unless otherwise stated. BCECF-AM, added at 5 μM in DMSO for loading the cells, was obtained from Merck KGaA, Darmstadt, Germany.

Pipette solutions were used as described below. For OHCs a high intracellular Cl^- was maintained to maximise the Cl^- gradient across the cell and to ensure that there was no run-down of chloride at the cytoplasmic surface of prestin in the OHC basolateral membrane. For CHO cells the intracellular Cl^- was kept at 11 mM using aspartate as the counter anion.

Salicylate, a weak acid which can modify pH_i (Tunstall *et al.* 1995), was applied in the extracellular solutions in some experiments. Sufficient initial time was allowed for pH_i to equilibrate before measurements were made.

Electrophysiology

Electrophysiological recordings were carried out at room temperature (20–22°C). Experiments on cochlear OHCs were carried out using conventional patch-clamp techniques as reported previously, using pipettes containing (in mM): K, 140; Cl 142; Mg, 1; Hepes, 5; EGTA, 1; and tritrated to pH 7.3 with KOH. Experiments on CHO cells were carried out 2–3 days after transfection. Recordings were made in the tight-seal, whole-cell configuration or in a perforated-patch configuration when 100 $\mu g\ ml^{-1}$ gramicidin was added in the pipette. Pipettes

were made from borosilicate glass (bath impedance 3–5 MΩ) and filled with (in mM): potassium aspartate, 130; NaCl, 10; Hepes, 5; Na_2ATP, 3; EGTA, 1; $MgCl_2$, 0.5; titrated to pH 7.4 with KOH. For non-linear capacitance measurements, CsCl replaced KCl in the pipette solution to minimise any background potassium currents. Patch currents were recorded using an Axopatch 200B amplifier (Axon Instruments, CA, USA) with 60–90% series resistance compensation and then digitised at 5 kHz. Liquid junction potentials were corrected off-line and data were analysed using Origin software (OriginLab, MA, USA). No series resistance compensation was applied for reversal potential experiments. An agar bridge contacting an AgCl electrode was used as reference electrode to minimize electrode offset and drift over the time course of the all the experiments.

Prestin–pHluorin non-linear capacitance

Non-linear capacitance was recorded in HEK293 cells in whole-cell mode using a lock in amplifier for piecewise linear capacitance measurement at a frequency of 800 Hz. A 10 mV sine wave command was summed with a 1 s ramp −150 to +100 mV. Data were fitted by the derivative of a Boltzmann function to obtain potential at peak, $V_{1/2}$ and slope parameter α, as described previously (Chambard & Ashmore, 2003). The intracellular pipette medium included caesium to block the additional baseline current in HEK cells and contained (in mM): CsCl, 140; Hepes, 10; EGTA 0.5, pH 7.3. The extracellular medium was constituted as above and buffered with Hepes or bicarbonate as appropriate.

Imaging of pH fluorescence

Images were captured on an inverted microscope (Axiovert S-100, Carl Zeiss, Germany) using a FLUAR 40× 1.3 NA oil objective. Images were acquired at 0.1 Hz using a CCD camera with 12-bit fluorescence resolution (PCO Sensicam, Photon Lines, UK) and processed using IQ software (Andor Technology, UK). GFP fluorescence was identified using an FITC filter set. The probes were excited at 470 nm (pHluorin) or as a ratiometric pair 440/490 nm (BCECF) using a Polychrome V monochromatic light source (TILL Photonics, Germany). The emission was measured at 530 nm. The intensity of the exciting light was reduced as much as possible to minimize photobleaching whilst maintaining a good signal-to-noise level. The relationship between the pH_i change and intracellular fluorescence change was calibrated for small perturbations using a weak acid/base method (Szatkowski & Thomas, 1986; Eisner *et al.* 1989), or more conventionally using the protonophore nigericin and different calibrated external pH solutions. The fluorescence data were analysed using IQ (Andor Technology) or ImageJ (NIH, USA) and the fitting carried out using Origin and Matlab software (The MathWorks Inc., Natick, MA, USA).

Computational simulations

Model simulations of CO_2 and HCO_3^- transmembrane fluxes into CHO cells, based on equations 8a and 9a of Boron & De Weer (1976), were carried out to confirm the pH time course. Programs were rewritten in Matlab using an appropriate solver, ode23s, for the (stiff) ordinary differential equations.

In data presentation, values are mean ± SEM unless otherwise stated. Significance where appropriate was evaluated with a Student's *t* test.

Results

Outer hair cell responses to bicarbonate

Most experiments on isolated mammalian OHCs are conducted in media with extracellular pH buffering using Hepes, as this buffer allows extracellular cations to be manipulated over a great range. Guinea-pig OHCs can be maintained and recorded when the perfusing solution contains bicarbonate as the pH buffer except that the difficulty of maintaining this buffer environment in a small chamber has discouraged its regular use. In some reported experiments phosphate-buffered media have also been used (e.g. Housley & Ashmore, 1992) as, in general, such solutions keep the cells usable for longer periods of time. To investigate the effect of bicarbonate, the endogenous *in vivo* buffer, experiments were carried out on isolated OHCs where the external pH buffer was changed by superfusion. Figure 1 shows an experiment where the internal pH and OHC length were monitored by preloading the cell with 5 μM BCECF-AM and the cell exposed to physiological levels of bicarbonate. As described previously (Ikeda *et al.* 1992), bicarbonate in the presence of low external chloride produced an initial acidification followed by a slow regulation of pH_i back to normal levels. The initial acidification has been ascribed to entry of CO_2 across the OHC membrane, but the pH recovery is due to bicarbonate loading from the extracellular solution.

Length changes in the cell were measured by tracking the ends of the cell in the sequence of images. The data showed that the addition of bicarbonate produced a small length increase, a finding compatible with the entry of bicarbonate into the cell (Fig. 1). There was no length change during the acidification, suggesting that any gas exchange was osmotically neutral. However, when the cell was initially perfused with 5 mM external chloride, but in the continued presence of Hepes, there was a rapid, transient shortening. Similar observations have

been reported in the presence of non-bicarbonate buffers (Cecola & Bobbin, 1992), but with no clear explanation. The simplest hypothesis is that, initially chloride can leave the cell but with no pH change and that the consequent volume reduction is responsible for the length increase. The transient nature of this response is less clear and may be due to re-equilibration of anions across the membrane. The pH changes indicated by the changing BCECF fluorescence ratio are, however, compatible with the presence of a bicarbonate–chloride exchanger in the OHC lateral membrane (Ikeda *et al*. 1992). These were explored further in the heterologous expression system experiments below.

OHC ionic currents in the presence of bicarbonate

Figure 2 shows that, in OHCs in low external chloride (Cl_o), addition of external bicarbonate produced a small inward current around the resting potential. The experiment was conducted using organ of Corti strips (see Methods) in which single OHC currents were recorded by whole-cell tight-seal recording. The experiment started by first switching to low Cl_o to reduce any subsequent liquid junction potential (LJP) effects, a prominent complication of anion substitution experiments arising from the lower mobility of gluconate compared with chloride. The LJP between normal (146 mM) and low Cl_o (1 mM) was calculated to produce a depolarization of the cell by 13.2 mV. This difference from the nominal command was corrected offline. A lowered Cl_o also reduced the outward current (above −20 mV), as has been noted in other systems. The effect may arise from the change in the titration of a surface positive charge at the pore of the K^+ channels (Frace *et al.* 1992).

On replacing Hepes buffer with 23 mM bicarbonate in 1 mM Cl_o the slope of the *I–V* curve negative to −50 mV was reduced. In this example the *I–V* curves obtained in low Cl_o–Hepes and low Cl_o–bicarbonate crossed at about −90 mV and produced a small negative shift (−10 mV) in the zero current crossing. Similar effects were seen in three other cells studied from more basal locations in turn 3 (data not shown). Although some of the slope reduction may be ascribed to intracellular protons competing with Ca^{2+} for binding at K_{Ca} channels in OHCs, the negative shift of the *I–V* intercept is consistent with a net inwardly directed current arising from anion movements. Without

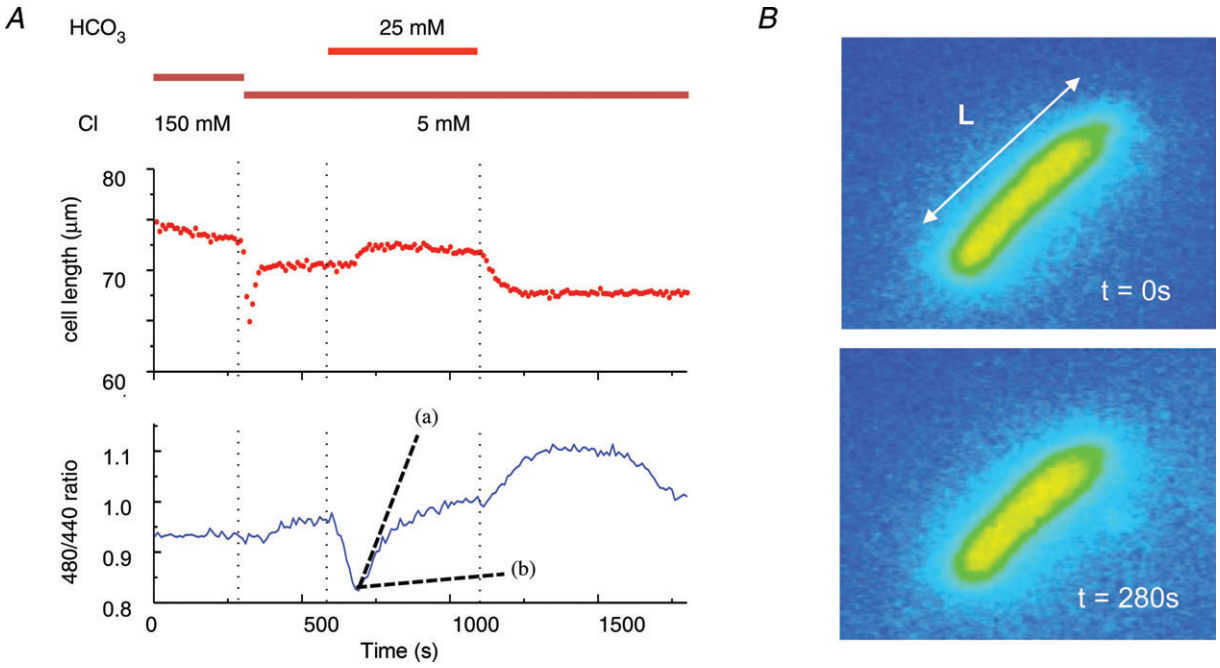

Figure 1. Effect of bicarbonate in isolated guinea-pig OHCs
A, extracellular chloride and bicarbonate affect OHC pH_i and length. The starting solution was buffered by 10 mM Hepes and 25 mM HCO_3^- replacement introduced by superfusion of the bath. The introduction of bicarbonate led to a transient acidification (shown by the change in the BCECF fluorescence ratio) followed by recovery on bicarbonate loading. The slope of this recovery (shown as a dashed line (a)) is to be compared with the slope (shown as dashed line (b)) estimated for OHCs exposed to 25 mM HCO_3^- in 150 mM Cl_o^- (reported by Ikeda *et al*. 1992, Fig. 11 and converted to a ratio as in Tunstall *et al*. 1995). On removal of bicarbonate the pH overshot the baseline. There was a transient OHC shortening on first moving to low Cl_o shown at 280 s. The cells recovered to a steady length with a small increase in length, L, during HCO_3^- application. *B*, frames showing an OHC loaded with BCECF, monitored during bath solution exchange at time points $t = 0$ and $t = 280$ s. Widefield fluorescent microscopy.

further cation channel block, it is difficult to disentangle anion movement from background current changes. No significant qualitative differences were noted between the K^+ currents measured in the presence of bicarbonate buffer or Hepes buffer (data not shown). The data in Figs 1 and 2, taken together with previous published data (e.g. Ikeda *et al.* 1992), suggest that prestin may exhibit the properties of a weak anion–bicarbonate exchanger. To further explore this hypothesis, experiments were carried out using heterologous expression systems where the effects of K^+ channel expression could be minimised.

Prestin–pHluorin in an expression system

To detect bicarbonate movement specifically mediated by prestin, sensitivity to intracellular pH changes near the membrane was enhanced by using the fluorescent sensor protein pHluorin at the membrane of an expression system. Figure 3 shows how pHluorin was used to operate as a pH_i sensor when fused to the prestin protein and expressed in transfected CHO cells. Cells successfully transfected were identified by a pronounced fluorescent ring, typical for membrane-targeted proteins, and are shown in Fig. 3*A*. The panels show cells transfected with prestin–pHluorin and with a membrane-anchored pHluorin (but without prestin) under the viewing conditions used in the experiments.

We first determined that fusing pHluorin to prestin did not perturb the electrical signature of prestin. It should be noted that no effect of GFP fusion to prestin has been reported in numerous studies on non-linear capacitance (e.g. Oliver *et al.* 2001). Here, the non-linear capacitance of prestin–pHluorin expressed in HEK293 cells was measured conventionally. The value of $V_{1/2}$, the potential at the peak non-linear capacitance and α, the slope of the underlying Boltzmann function were respectively -41 ± 18 mV and 43 ± 4 mV^{-1} (SD, $n = 5$). Although scatter in $V_{1/2}$ is known to arise from different metabolic states of the cell (Frolenkov *et al.* 2000), the data were not significantly different from values reported elsewhere for prestin (Oliver *et al.* 2001). In 1 mM Cl^-–25 mM HCO_3^- extracellular solution, the $V_{1/2}$ and α values remained unchanged (-48 ± 25 mV and 42 ± 17 mV^{-1}, respectively) compatible with the Cl_o insensitivity of the prestin non-linear capacitance. The results thus indicate that prestin–pHluorin retains the electrical gating charge characterising the native prestin protein.

In order to measure the pH dependence of the intracellular pHluorin signal, the fluorescence from the membrane was calibrated using two methods: (1) using

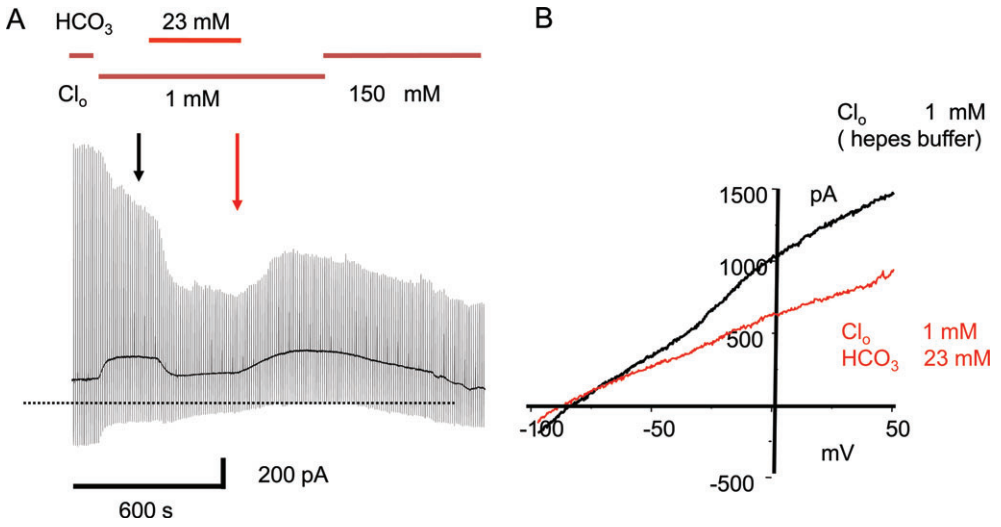

Figure 2. Extracellular chloride and bicarbonate affect guinea-pig OHC *I–V* curves
A, Cl_o was reduced from 150 mM to 1 mM Cl_o (Hepes buffered) at the start of the experiment. 25 mM HCO_3^- replaced the Hepes buffer solution as shown. The OHC, in an organ of Corti strip preparation, was held under whole-cell recording conditions at −60 mV and 1 s voltage ramps from −85 to +50 mV applied every 10 s to obtain the *I–V* curves. *B*, *I–V* curves selected in low Cl_o just before and at the end of the HCO_3^- application. 25 mM HCO_3^- added in 1 mM Cl_o reduced the slope of the *I–V* curves at hyperpolarized potentials and produced a negative shift in the zero-current reversal potential. The reduction in the outward current at depolarized potentials was reversible on removal of HCO_3^-. The initial change from 150 mM Cl_o to 1 mM Cl_o produced a positive shift in the holding current due to the effect of the liquid junction potential (LJP). The LJP produced an effective shift of +13.2 mV in the nominal holding potential and has been corrected in the *I–V* curves. The computed liquid junction potential shift due to Hepes–HCO_3^- exchange was +0.5 mV and no further correction was required. Over the 30 min recording period there was a steady decline in outward current probably due the effect of prolonged low Cl_o, as short Cl_o exposures produced reversible outward current reduction (data not shown).

a modified method of Szatkowsky and Thomas (Eisner *et al.* 1989), and (2) using a conventional method where the membrane was permeabilized using nigericin. In method 1, it is assumed that the relationship between changes in pH_i and changes in fluorescence is linear in the experimental range. The proportionality constant can therefore be determined from measurements of changes in fluorescence for different concentrations of weak base and weak acid. Figure 3*C* shows the fluorescence of pHluorin measured upon addition of trimethylamine (TMA, a weak base) and butyric acid (BA, a weak acid) at the concentrations shown. The figure indicates that addition of trimethylamine led to an increase of the pHluorin signal due to intracellular alkalinisation. Conversely, addition of butyrate reduced the fluorescence as the intracellular compartment acidified. From such measurements it was calculated that 10% change in the fluorescence around pH 7.3 corresponds to a change in pH of 0.26 ± 0.06 ($n = 33$).

In the second method, nigericin (10 μM) was used in the bath and a series of independently calibrated pH solutions applied in sequence. For the range of interest, a piecewise linear fit to the data around pH 7.3 gave a value of 10% change in fluorescence which corresponds to a change of 0.31 pH units, in reasonable agreement with the acid/base method. For the considerations below this linear relation will be used to estimate pH_i.

The fluorescence signal calibrated from the recombinant prestin–pHluorin protein is shown in Fig. 3*D*. On application of 25 mM HCO_3^- equilibrated with 5% CO_2 (corresponding to a dissolved concentration of 1.3 mM), the cell typically acidified by 0.9 pH unit. This result can be interpreted as arising from the passive influx of CO_2 from the bath leading to the production of intracellular H_2CO_3. There was little pH_i regulation under these experimental conditions. After pH_i re-equilibrated to near its original value, the extracellular solution was replaced isotonically with one including 50 mM ammonium, leading to intracellular alkalinisation as result of the NH_3 influx. The alkalinisation recovered slowly. These data show that the recombinant prestin–pHluorin protein can be used to monitor the changes in pH_i near the membrane and give a quantitative estimate of the pH change.

Figure 4 shows the experimental protocol used to investigate the ability of prestin to transport HCO_3^-. The protocol relied on the measurement of pH_i recovery from a CO_2-induced acidification in the presence of extracellular

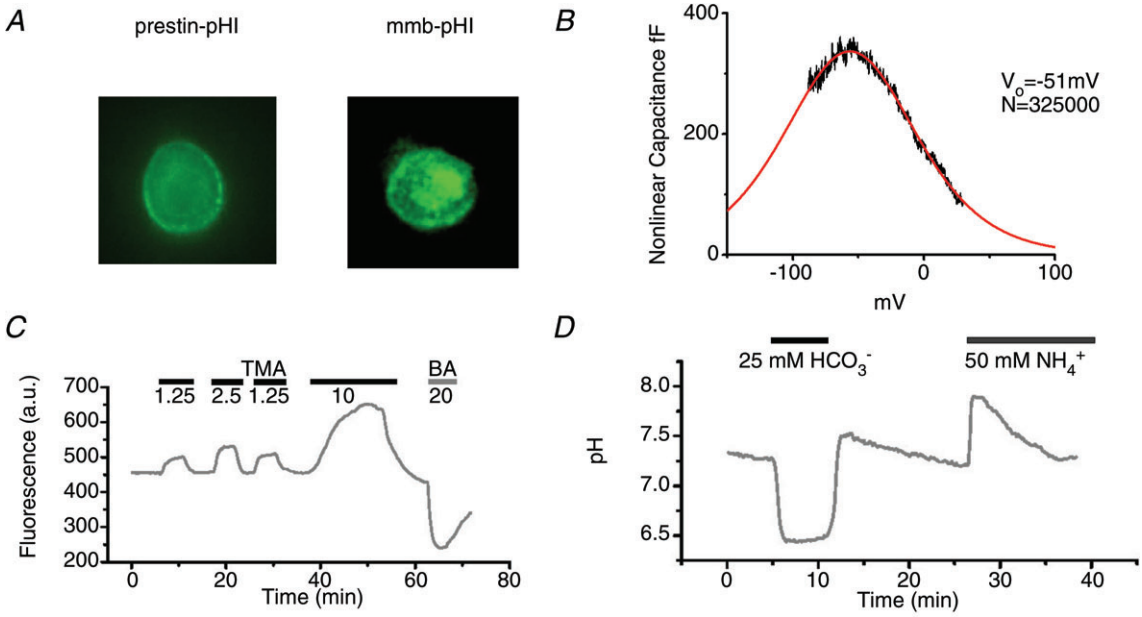

Figure 3. Recombinant prestin–pHluorin protein as a pH_i sensor in CHO cells
A, expression pattern of the prestin–pHluorin protein in CHO cells (prestin–pHl) and membrane–pHluorin (mmb–pHl) as the control. Both wide-field images from experimental sequences show predominant membrane localisation of the label. These membrane regions were analysed for the data shown in subsequent figures. *B*, non-linear capacitance trace of a CHO cell identified by its pHluorin fluorescence pattern. The continuous curve is the fitted derivative of a Boltzmann curve $C_{NL} = 4\ C_{max}\ \Phi_B(1 - \Phi_B)$ where $\Phi_B = 1/(1 + \exp(\beta(V - V_o))$ and $\beta = 1/43$ mV and $V_o = -51$ mV. The number of equivalent charge carriers, N, was calculated to be 3.25×10^5 (Chambard & Ashmore, 2003). *C*, calibration of raw fluorescence data using modified method of Szatkowsky and Thomas (see Methods). The trace shows the pHluorin signal with excitation at 470 nm and emission above 510 nm. Solutions shown with concentrations (in mM) of trimethylamine (TMA) or butyrate acid (BA) were applied as indicated. *D*, time course of the pH-calibrated pHluorin signal. Extracellular solutions containing 25 mM HCO_3^- equilibrated with 5% CO_2 or 50 mM NH_4^+ were applied at the times indicated.

25 mM HCO_3^-. A typical time course of the fluorescence signal from a cell transfected with prestin–pHluorin is shown. A cell transfected with membrane-targeted pHluorin acted as a control (Fig. 4*A*). The data show that in the presence of high Cl_o (146 mM), the pH_i recovery rate was slight. The slow kinetics did not allow an accurate determination of the recovery time constant and therefore the initial rate of pH_i recovery was measured from the linear fit of the initial segment of the pH_i response instead. In a population of 28 cells, the recovery rate was 0.023 ± 0.006 pH units min^{-1}. No significant differences in the measurable prestin-dependent bicarbonate transport were observed between transfected and untransfected cells.

After reducing the external chloride concentration to 6 mM, the recovery in a cell expressing recombinant prestin–pHluorin protein was much faster. Indeed, the pH_i recovery rate was found to be approximately 4 times larger in the presence of prestin (0.106 ± 0.028 *vs.* 0.030 ± 0.003 pH units min^{-1}, $n = 6$ and 22, respectively) and was statistically significant (Fig. 4*B*). These data indicate that prestin can transport HCO_3^- into the cell (i.e. it is an alkali loader) but that low Cl_o is required. The results thus indicate, as implied from the OHC experiments above and as reported previously (Ikeda *et al.* 1992), that in prestin-transfected cells HCO_3^- and Cl^- fluxes are coupled and that these fluxes can control pH_i.

Salicylate is a known blocker of the non-linear capacitance exhibited by prestin, with an estimated $K_i = 200\ \mu$M on the intracellar surface (Oliver *et al.* 2001). Application of 10 mM salicylate applied in the bath was found to slow the pH_i recovery in low Cl_o (6 mM). In transfected cells, salicylate slowed the pH_i recovery from 0.106 ± 0.028 pH units min^{-1} induced by low chloride/bicarbonate to 0.042 ± 0.010 pH units min^{-1}. Salicylate had no significant effect when Cl_o was high (146 mM) (data not shown). Although the data are consistent with inhibition of a Cl^-–HCO_3^- exchange, salicylate itself is a weak acid (Tunstall *et al.* 1995) and the effect is therefore more complex to analyse than a simple inhibitory effect on the transporter.

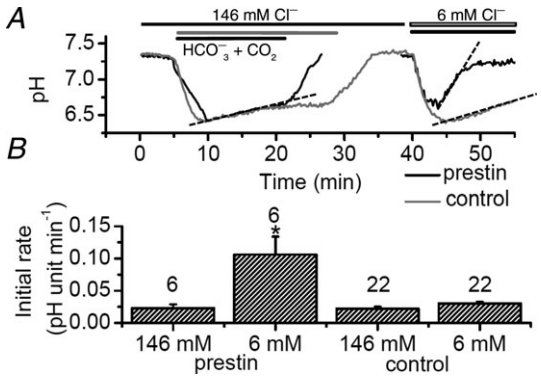

Figure 4. Prestin enhances the recovery of intracellular pH from acidification
A, typical time course of pHluorin fluorescence from a CHO cell expressing prestin–pHluorin and a control cell with mmb–pHluorin construct anchored intracellularly in the membrane. 25 mM HCO_3^- equilibrated with 5% CO_2 was added extracellularly either in the presence of $[Cl^-]_o = 146$ or 6 mM. Different application times used in the two experiments are indicated. *B*, the initial rates of pH_i recovery obtained by a linear fit of the corresponding data regions in *A*. Rates shown on the figures for $[Cl^-]_o = 146$ mM. For prestin-positive cells the initial rate was 0.023 ± 0.006 pH unit min^{-1}; for prestin-negative cells, the initial rate was 0.022 ± 0.003 pH unit min^{-1}; for $[Cl^-]_o = 6$ mM, the rates were 0.106 ± 0.028 and 0.030 ± 0.003 pH unit min^{-1} for prestin-positive and prestin-negative cells, respectively. Dashed lines show measured slopes. Numbers of cells indicated by data bars. *Significant difference in recovery slopes between prestin–pHluorin and mmb–pHluorin transfected cells measured in 6 mM Cl_o ($P < 0.05$).

Imaging CHO cells with BCECF

The pH_i recovery produced by HCO_3^- loading was monitored independently using a cytoplasmic pH-sensitive dye, BCECF (Fig. 5). DNA encoding prestin–GFP rather than prestin–pHluorin was used in this set of experiments to identify transfected cells readily. Two transfected cells are shown in Fig. 5*A*, before and after loading by 5 μM BCECF-AM. Cells without GFP signal in the same imaging frame were used as controls. The

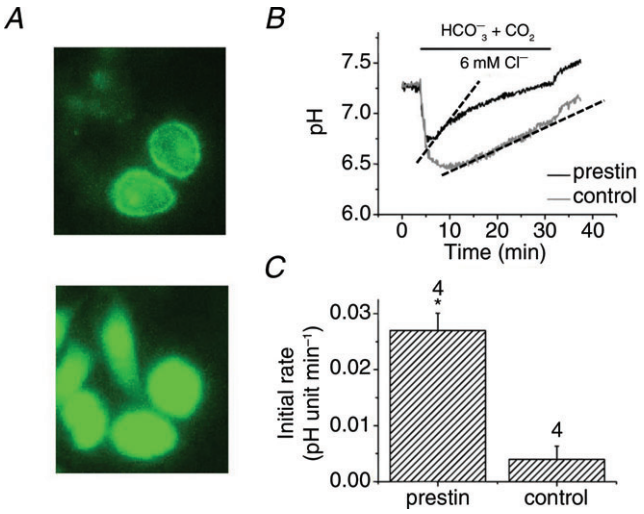

Figure 5. Intracellular acidification monitored using BCECF
A, a field of cells transfected with prestin–GFP (top) and the same field after all cells were loaded with BCECF using the AM ester (bottom). *B*, superimposition of the time course of pH_i recovery in a transfected and untransfected cells. *C*, initial rates of recovery calculated from *B* as calibrated in Fig. 3: 0.027 ± 0.003 and 0.004 ± 0.002 pH units min^{-1}, in transfected and untransfected cells, respectively. Dashed lines show measured slopes. Numbers of cells indicated by data bars. *Significant difference from untransfected cells ($P < 0.05$).

simultaneous overlay of the pH_i time course obtained from transfected and untransfected cells is shown in Fig. 5*B*. The comparison indicated that, in this case also, the recovery was significantly faster in prestin-positive cells compared with controls (0.027 ± 0.003 ($n = 4$) and 0.004 ± 0.002 ($n = 4$) pH units min^{-1}, respectively. The results are summarised in Fig. 5*C*. The data show that the expression of prestin leads to a change of pH_i in the cell cytoplasm. The simplest interpretation of the slower pH_i recovery in these experiments compared with prestin–pHluorin is that BCECF had a different distribution within the cell compared with prestin–pHluorin. BCECF would not have detected near-membrane pH_i changes possible with the pHluorin probes.

Effect of prestin on the electrical properties of CHO cells

To investigate a possible electrogenicity of Cl^--dependent HCO_3^- transport, we compared the current–voltage characteristics (*I–V* curve) in untransfected and transfected cells by changing Cl_o in the presence of bicarbonate. A HCO_3^-:Cl^- stoichiometry of 1:1 would present no changes in the cell's electrical properties when transport is activated but any other stoichiometry would have measurable effects on the *I–V* and in particular on the zero current potential, V_R.

Figure 6 shows the *I–V* curves determined by whole-cell recording, in the continuous presence of 25 mM extracellular HCO_3^-. When $[Cl^-]_o = 146$ mM there was no significant difference in V_R between untransfected and transfected cells ($V_R = -45 \pm 2$ ($n = 6$) *vs.* -51 ± 4 mV ($n = 5$), respectively). When Cl_o was lowered to 2 mM the intercept shifted positively by 21 mV in untransfected cells (to $V_R = -24 \pm 3$, $n = 5$), but shifted negatively by 24 mV in transfected cells (to $V_R = -75 \pm 10$ mV ($n = 6$)). Figure 6*C* and *D* show the complete sets of data for untransfected and transfected cells, respectively. Although residual ionic currents in the cells make these shifts relative measurements, the differences between the

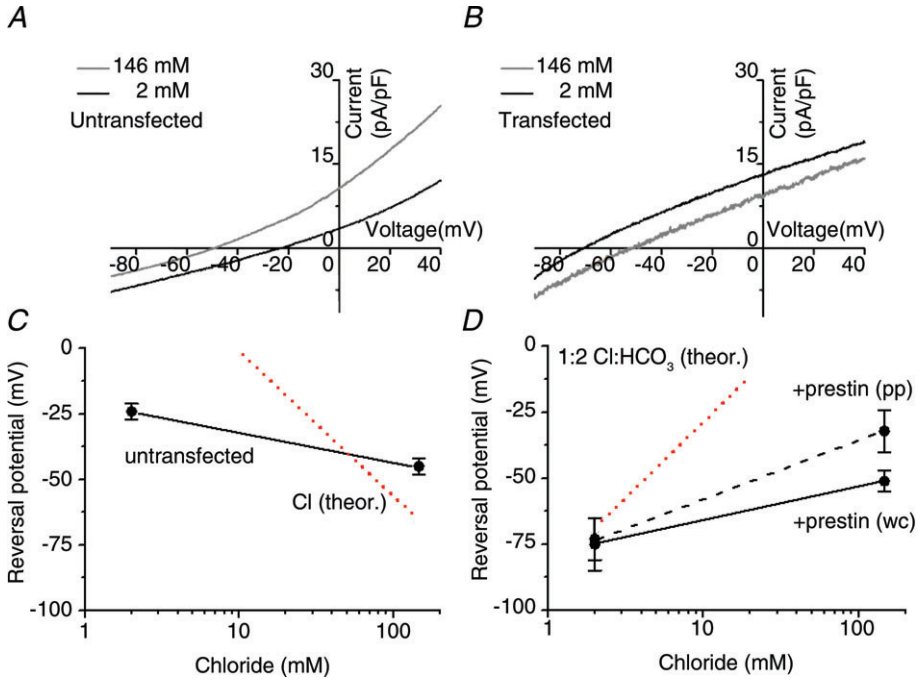

Figure 6. Extracellular chloride affects the *I–V* of prestin-transfected CHO cells
Current–voltage (*I–V*) characteristics from *A*, an untransfected and *B*, a prestin-transfected CHO cell. A voltage ramp from −90 to +40 mV was used to generate the *I–V* curves and the zero current potential, V_R, was determined from the current curve intercept. The whole-cell recordings used $[Cl^-]_i = 11$ mM in the pipette (see Methods). 25 mM HCO_3^- equilibrated with CO_2 was present throughout. *C*, V_R for untransfected cells. In 2 mM Cl_o, $V_R = -24 \pm 3$ mV ($n = 6$) and in 146 mM Cl_o $V_R = -45 \pm 3$ mV ($n = 6$). The dotted line shows the (Nernstian) prediction for a simple chloride electrode when the internal chloride, $Cl_i = 11$ mM. No further correction for leak currents has been carried out to align the experimental data with the theoretical predictions. *D*, V_R for prestin-transfected cells. In the whole-cell (wc) recording configuration and in 2 mM Cl_o, $V_R = -75 \pm 10$ mV ($n = 5$); in 146 mM Cl_o, $V_R = -51 \pm 4$ mV ($n = 5$). In the perforated patch (pp) configuration and in 2 mM Cl_o, $V_R = -73 \pm 8$ mV ($n = 7$); in 146 mM Cl_o, $V_R = -32 \pm 8$ mV ($n = 7$). The dotted line shows the theoretical prediction for V_R for an antiporter with a 1:2 Cl^-:HCO_3^- stoichiometry derived from eqn (1) using $[Cl^-]_i = 11$ mM and $[HCO_3^-]_i = 15$ mM. A stoichiometry of 2:1 Cl:HCO_3 would result in a line with a negative slope, −58 mV per decade.

two populations of cell strongly suggest that prestin transport controls electrical properties of the cell membrane, i.e. the transport activity is electrogenic.

Recordings were also made in prestin-transfected cells using perforated-patch recordings with gramicidin as the ionophore to maintain intact $[Cl^-]_i$. The data have been added to Fig 6*D*. Lowering Cl_o from 146 to 2 mM produced a negative shift of 41 mV in V_R (from -32 ± 7 mV to -73 ± 8 mV ($n = 7$)). This shift was in the same direction as found in the whole-cell configuration, although slightly larger suggesting that whole-cell recording may have lowered Cl_i. We conclude that the zero current potential V_R was ~−75 mV in transfected CHO cells when $[Cl^-]_o = 2$ mM, independent of the recording configuration.

The predictions for an antiporter with the various stoichiometries can be made in the steady state from thermodynamic considerations (De Weer *et al.* 1988; Schaechinger & Oliver, 2007). If the transporter turnover is *m* Cl:*n* HCO_3 (with *m* and *n* not equal), the zero current potential V_R is given by

$$V_R = (m\,E_{Cl} - n\,E_{HCO_3})/(m - n) \qquad (1)$$

where E_X is the Nernstian equilibrium potential of the species. The predictions for V_R as well as in the case where the equilibrium is dominated by a simple Cl^- conductance is shown in Fig. 6*C* and *D*. Both a simple, constant Cl^- permeability as well as a 2 Cl^-:1 HCO_3^- antiporter activity predict a positive shift in V_R when Cl_o is lowered. However, a 1 Cl^-:2 HCO_3^- stoichiometry predicts a negative shift ('non-Nernstian' behaviour). Equation (1) shows that $\Delta V = -\Delta E_{Cl}$ and in this case the expected zero current potential shifts negatively when Cl_o is lowered. In the case that the intracellular chloride concentration remains constant (as it would, approximately, were the cell to be recorded in the whole-cell configuration) the predicted shift $\Delta V = 25 \log_e (2/146) = -107$ mV. At normal Cl_o (146 mM) the zero current potential, V_R, of the measured *I–V* values would be controlled by any residual endogenous currents which were not determined in these experiments, and their presence would account for deviations from eqn (1). Nevertheless, Fig. 6*C* and *D* shows that the zero current potentials, V_R, in transfected and untransfected cells in normal Cl_o were similar. Therefore, prestin transfection did not substantially alter the basal electrical membrane properties of the cells.

In order to measure the interrelation between pH and V_R, Fig. 7 shows an experiment when the fluorescence signal from prestin-transfected cells was followed during measurement of the reversal potential in the whole-cell configuration. The time course of fluorescence signal showed that a reduction in Cl_o from 146 to 2 mM in the presence of extracellular 25 mM HCO_3^- was necessary to activate the pH_i recovery. This observation confirms that the alkalinisation of intracellular space requires an (outward) Cl^- gradient across the membrane and that the transport of HCO_3^- and Cl^- are coupled. A similar time course was obtained from three cells. The steady-state values of the zero current potential (-75 ± 10 mV and -51 ± 4 mV for $[Cl^-]_o = 2$ and 146 mM, respectively, from $n = 6$ cells) are shown for comparison.

Discussion

The data show that a pH-sensitive fluorescence probe, superecliptic pHluorin (Miesenbock *et al.* 1998), can be used to measure intracellular pH in close proximity to prestin in the cell membrane. This recombinant construct is similar to that where GFP is attached to prestin's C-terminal end and routinely used for the functional analysis of prestin in many other studies (Oliver *et al.* 2001; Chambard & Ashmore, 2003; Schaechinger & Oliver, 2007).

The strategy of covalently linking the probe with the protein provides important advantages over a cytosolic pH indicator such as BCECF although such an experiment can be performed (Fig. 5). Firstly, the use of pHluorin does not require coexpression of a transfection-indicator such as GFP and thus the fluorescence signal from the pH sensor is not mixed with contributions from GFP. Secondly, such a membrane-anchored sensor detects pH changes only in a close proximity to prestin and not in a whole cellular volume and thus enhances the detectability of pH changes without loss of sensitivity due to volume

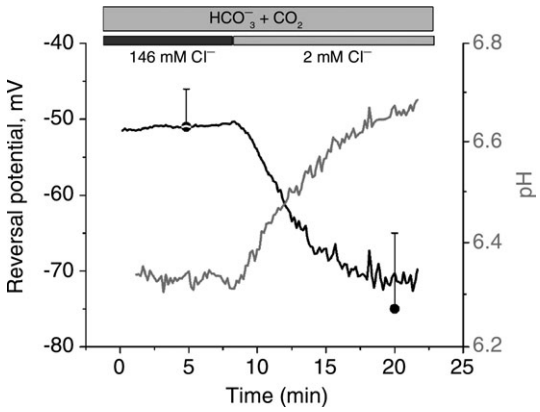

Figure 7. Interdependence of the Cl^- gradient and the reversal potential during HCO_3^- transport across the membrane
Intracellular pH and reversal potential were determined simultaneously from a cell expressing the recombinant prestin–pHluorin protein. Zero current reversal potential, V_R was determined from the *I–V* curve of the type shown in Fig. 6. The extracellular Cl^- was reduced from 146 mM to 2 mM in the presence of 25 mM HCO_3^- at the time indicated in the figure. $V_R = -51 \pm 4$ mV and -75 ± 10 mV for $[Cl^-]_o = 146$ mM and 2 mM, respectively ($n = 5$).

dilutions. Such approach is well suited for a detection of small, spatially constrained changes in pH_i around prestin molecules.

The pH_i near the membrane was analysed by measuring the initial rate of pH_i recovery from a CO_2-induced intracellular acidification. It was shown that pH_i recovered 4 times faster in cells transfected with prestin, but only in the presence of low Cl_o and extracellular HCO_3^-. However, such acceleration required Cl_o to be lowered (in the case here to 6 mM or less) to establish a Cl^- gradient before detectable HCO_3^- can be driven into the cell. These findings indicate that mammalian prestin is indeed able to transport HCO_3^- in exchange for Cl^-. This increases its similarities to other members of the SLC26 family, for example SLC26A3, SLC26A6 (Shcheynikov *et al.* 2006) and SLC26A7 (Petrovic *et al.* 2004), and may well point to its evolution from a metabolic pH regulator in non-mammalian hair cell systems.

Is prestin an 'incomplete transporter'?

The presence of prestin in the cell membrane increased the pH recovery rate by $0.106 - 0.030 = 0.076$ pH units min^{-1} (Fig. 4). This rate can be converted into an estimate for the turnover rate of the transporter. If we assume that CHO cells behave like open systems, allowing free diffusion of carbon dioxide, the buffering power of the cytoplasm due to the CO_2–bicarbonate system at equilibrium can be obtained from differentiation of the Henderson–Hasselbalch equation as $2.30 \times [HCO_3^-]_i = 2.30 \times 25$ mM $= 58$ mM (Roos & Boron, 1981). If the intrinsic buffering power, β_i, of the cell cytoplasm is taken to be 11 mM, similar to the value found in neurones (Amos & Richards, 1996) and close to the value of 14 mM reported for OHCs (Ikeda *et al.* 1992), the total buffering power would have been 69 mM and the influx of equivalent hydroxyl ions due to prestin would have been $69 \times 0.076/60 = 0.087$ mM s^{-1}. This clearly represents an upper bound. Taking the cell volume $V = 2$ pl, corresponding to a cell 15 μm in diameter, the influx would be equivalent to 1.05×10^8 hydroxyls s^{-1}. Since the number of carriers in a typical CHO cell, measured by capacitance methods, is approximately 250,000 (Chambard & Ashmore, 2003) and on each cycle two HCO_3^- ions are transported, we find that an upper bound for the turnover number for each transporter, under our experimental conditions, would have been $1.05 \times 10^8/2 \times 2.5 \times 10^5 = 209\ s^{-1}$ per prestin. This turnover is still over 3 orders of magnitude lower than the rate reported for the red blood cell AE1/SLC4A1 Cl^-/HCO_3^- transporter (Jay & Cantley, 1986) and so prestin must be considered as a weak exchanger rather than an incomplete transporter. The turnover estimate is, however, less than the maximum uptake rate ($3000\ s^{-1}$ per prestin) for transport of a fructose substrate estimated by CHO cell swelling (Chambard & Ashmore, 2003).

Modelling the effects of prestin on membrane permeability

A semi-quantitative insight into the regulation of intracellular pH by means of bicarbonate and CO_2 membrane permeabilities can be obtained from a simple model of the bicarbonate transport system. The model was originally formulated to describe pH changes in the squid axon (Boron & De Weer, 1976) but can be modified for a different surface-to-volume ratio of the CHO cells. In this latter version of the model, intracellular concentrations were controlled only by corresponding bicarbonate and CO_2 fluxes and by their membrane permeabilities ($P_{CO_3^-}$ and P_{CO_2}, respectively). The CO_2 permeability P_{CO_2} represents a passive transmembrane flux, while $P_{HCO_3^-}$ is determined by the flux through any of the bicarbonate membrane transporters. As the complete kinetics of the prestin transporter are not known in sufficient detail, the effect of a coupled Cl^- gradient can be implemented by controlling the magnitude of $P_{CO_3^-}$. The initial acidification of the cell arises through the instantaneous permeation of CO_2 when bicarbonate is applied, and the subsequent alkalinisation is a result of the cell loading with bicarbonate. The model is a two-compartment model which does not include the slow, rate-limiting step associated with the chloride off-rate for the antiporter (Muallem & Ashmore, 2006) nor the effect of HCO_3^- diffusion away from the membrane into the cytoplasm. However, since the rate of pH recovery is proportional, initially, to the inwardly directed HCO_3^- flux, it might be expected that the initial rate of change of pH should be proportional to $P_{CO_3^-}$.

To confirm such conclusions, we used physiologically reasonable values of $P_{CO_2} = 10^{-4}$ cm s^{-1} and a baseline bicarbonate permeability $P_{HCO_3^-} = 3 \times 10^{-7}$ cm s^{-1}. The surface-to-volume ratio, ρ, for a cell 15 μm in diameter was taken to be $4000\ cm^{-1}$ and the intracellular buffering power was decreased slightly to $\beta = 4$ mM to obtain the pH excursion observed in our experiments. Numerical simulations (data not shown) indicate that the increase in low chloride pH_i recovery rate by $(0.106 - 0.023)/(0.03 - 0.022) = 10$ times requires an increase in $P_{CO_3^-}$ by approximately the same factor. Hence the effect of prestin is to add an additional membrane permeability for HCO_3^- 9 times that of the endogenous transport system. As a result, prestin conferred substantial pH buffering on the CHO cells in these experiments. The much higher prestin expression levels in OHCs (by over an order of magnitude) may therefore indicate that prestin makes a significant contribution to pH_i buffering in OHCs.

The stoichiometry of the prestin transporter

The determination of the stoichiometry of the transporter from patch-clamp measurements was complicated by relatively small currents evoked by mammalian prestin even though the reduction of Cl_o from 146 to 6 mM in the presence of 25 mM HCO_3^- generated a hyperpolarising shift in V_R in cells expressing prestin. The shift could not be explained by the presence of a Cl^- conductance because a simple Cl^- conductance predicts a membrane depolarisation rather than the hyperpolarisation observed. A HCO_3^-/Cl^- transporter with a 1:*n* stoichiometry (where $n > 1$) would have similar effect. We conclude that the observed zero current potential $V_R = -75$ mV (when $[Cl^-]_i = 11$ mM and $[HCO_3^-]_o = 25$ mM) is most simply described by a 2:1 stoichiometry. This result suggests that the transport mechanism of mammalian prestin has the same charge stoichiometry as its non-mammalian orthologues (Schaechinger & Oliver, 2007), but transports two molecules of HCO_3^- instead of one SO_4^{2-} found in non-mammalian orthologues.

Prestin is the OHC specific Cl^-/HCO_3^- transporter

In mammalian outer hair cells, there is clear evidence for pH_i regulation (Fig. 1 and Ikeda *et al.* 1992). The case was made by Ikeda *et al.* that pH_i regulation in OHCs used a Cl^-/HCO_3^- transport mechanism even though prestin and the SLC26 family were unknown at the time. The mechanism was partially inhibited by 0.3 mM DIDS. The present results indicate that prestin is responsible for pH regulation in the mammalian (and perhaps other) hair cells, in which case prestin and its orthologues may have evolved as a component of sensory hair cell pH regulation. Indeed, pH mis-regulation has been implicated in the slow degeneration of OHCs in prestin knockout mice (Liberman *et al.* 2002). Through the regulation of two major anions, chloride and bicarbonate, prestin could thus play a significant role in the maintenance of osmotic and turgor pressures in OHCs and hence determine cell stiffness (He *et al.* 2003; Mellado Lagarde *et al.* 2008). Thus, OHC ionic homeostasis, cell micromechanics and Cl^-:HCO_3^- counterflow are probably intimately linked.

Multiple roles of prestin in OHCs

The experiments described above describe an inward directed flux of bicarbonate through prestin. Physiologically, the OHC exchanger, as in most transport systems, is likely to operate in both forward and reverse modes. In imaging configurations, intracellular chloride, Cl_i, levels are unknown although, by using prestin itself as the sensor, it has been estimated that $[Cl_i]$ in OHCs is below 10 mM (Santos-Sacchi *et al.* 2006) and therefore the chloride gradient is close to being in equilibrium at the OHC resting potential. Since *in vivo* the bicarbonate buffering in the organ of Corti suggests that the bicarbonate gradient across OHC membrane would be small, prestin in the intact cochlea is likely to be operating close to its electrogenic reversal potential, eqn (1). We therefore propose that prestin in OHCs may also be responsible for $[Cl_i]$ regulation at these low levels and thus could be involved in homeostatic control of the cochlear amplifier gain. The inferred binding constant of prestin for $[Cl_i] = 6$ mM (Oliver *et al.* 2001) so that even small changes in Cl_i could regulate the voltage sensitivity of prestin. *In vivo*, any bicarbonate flux would be determined by the metabolic state of the OHC, the respiration rate of the mitochondria in the cell (whose role, particularly at the lateral membrane, has yet to be clarified) and any acid–base balance determined by the high bicarbonate content of the endolymph (Couloigner *et al.* 1999) coupled to the high carbonic anhydrase activity at the cell apex (Okamura *et al.* 1996). An inward bicarbonate flux has the potential to reduce Cl_i in the small OHC volume formed by the shell around the cortical cytoskeleton just below the lateral plasma membrane. This volume is typically about 10 fl, or less than 1% of the total cell volume. Such a reduction in Cl_i would tend to reduce the gain of the prestin as an actuator. Conversely, reducing the inward flux, or even reversing it, for example by increasing the respiratory demand on the cell, would increase the submembrane Cl_i^- and increase the forces produced by the OHC in cochlear amplification.

References

Amos BJ & Richards CD (1996). Intrinsic hydrogen ion buffering in rat CNS neurones maintained in culture. *Exp Physiol* **81**, 261–271.

Ashmore J (2008). Cochlear outer hair cell motility. *Physiol Rev* **88**, 173–210.

Ashmore JF (1987). A fast motile response in guinea-pig outer hair cells: the cellular basis of the cochlear amplifier. *J Physiol* **388**, 323–347.

Bai JP, Surguchev A, Montoya S, Aronson PS, Santos-Sacchi J & Navaratnam D (2009). Prestin's anion transport and voltage-sensing capabilities are independent. *Biophys J* **96**, 3179–3186.

Boron WF & De Weer P (1976). Intracellular pH transients in squid giant axons caused by CO_2, NH_3, and metabolic inhibitors. *J Gen Physiol* **67**, 91–112.

Brownell WE, Bader CR, Bertrand D & de Ribaupierre Y (1985). Evoked mechanical responses of isolated cochlear outer hair cells. *Science* **227**, 194–196.

Cecola RP & Bobbin RP (1992). Lowering extracellular chloride concentration alters outer hair cell shape. *Hear Res* **61**, 65–72.

Chambard JM & Ashmore JF (2003). Sugar transport by mammalian members of the SLC26 superfamily of anion-bicarbonate exchangers. *J Physiol* **550**, 667–677.

Couloigner V, Teixeira M, Sterkers O & Ferrary E (1999). *In vivo* study of the electrochemical composition of luminal fluid in the guinea pig endolymphatic sac. *Acta Otolaryngol* **119**, 200–202.

Cross FR, Garber EA, Pellman D & Hanafusa H (1984). A short sequence in the p60src N terminus is required for p60src myristylation and membrane association and for cell transformation. *Mol Cell Biol* **4**, 1834–1842.

Dallos P (2008). Cochlear amplification, outer hair cells and prestin. *Curr Opin Neurobiol* **18**, 370–376.

De Weer P, Gadsby DC & Rakowski RF (1988). Voltage dependence of the Na-K pump. *Annu Rev Physiol* **50**, 225–241.

Dorwart MR, Shcheynikov N, Yang D & Muallem S (2008). The solute carrier 26 family of proteins in epithelial ion transport. *Physiology (Bethesda)* **23**, 104–114.

Eisner DA, Kenning NA, O'Neill SC, Pocock G, Richards CD & Valdeolmillos M (1989). A novel method for absolute calibration of intracellular pH indicators. *Pflugers Arch* **413**, 553–558.

Frace AM, Maruoka F & Noma A (1992). Control of the hyperpolarization-activated cation current by external anions in rabbit sino-atrial node cells. *J Physiol* **453**, 307–318.

Frank G, Hemmert W & Gummer AW (1999). Limiting dynamics of high-frequency electromechanical transduction of outer hair cells. *Proc Natl Acad Sci U S A* **96**, 4420–4425.

Frolenkov GI, Mammano F, Belyantseva IA, Coling D & Kachar B (2000). Two distinct Ca^{2+}-dependent signaling pathways regulate the motor output of cochlear outer hair cells. *J Neurosci* **20**, 5940–5948.

Géleoc GS, Casalotti SO, Forge A & Ashmore JF (1999). A sugar transporter as a candidate for the outer hair cell motor. *Nat Neurosci* **2**, 713–719.

He DZ, Jia S & Dallos P (2003). Prestin and the dynamic stiffness of cochlear outer hair cells. *J Neurosci* **23**, 9089–9096.

Housley GD & Ashmore JF (1992). Ionic currents of outer hair cells isolated from the guinea-pig cochlea. *J Physiol* **448**, 73–98.

Ikeda K, Saito Y, Nishiyama A & Takasaka T (1992). Intracellular pH regulation in isolated cochlear outer hair cells of the guinea-pig. *J Physiol* **447**, 627–648.

Jay D & Cantley L (1986). Structural aspects of the red cell anion exchange protein. *Annu Rev Biochem* **55**, 511–538.

Johnson SL, Beurg M, Marcotti W & Fettiplace R (2011). Prestin-driven cochlear amplification is not limited by the outer hair cell membrane time constant. *Neuron* **70**, 1143–1154.

Kachar B, Brownell WE, Altschuler R & Fex J (1986). Electrokinetic shape changes of cochlear outer hair cells. *Nature* **322**, 365–368.

Liberman MC, Gao J, He DZ, Wu X, Jia S & Zuo J (2002). Prestin is required for electromotility of the outer hair cell and for the cochlear amplifier. *Nature* **419**, 300–304.

Mellado Lagarde MM, Drexl M, Lukashkin AN, Zuo J & Russell IJ (2008). Prestin's role in cochlear frequency tuning and transmission of mechanical responses to neural excitation. *Curr Biol* **18**, 200–202.

Miesenbock G, De Angelis DA & Rothman JE (1998). Visualizing secretion and synaptic transmission with pH-sensitive green fluorescent proteins. *Nature* **394**, 192–195.

Muallem D & Ashmore J (2006). An anion antiporter model of prestin, the outer hair cell motor protein. *Biophys J* **90**, 4035–4045.

Okamura HO, Sugai N, Suzuki K & Ohtani I (1996). Enzyme-histochemical localization of carbonic anhydrase in the inner ear of the guinea pig and several improvements of the technique. *Histochem Cell Biol* **106**, 425–430.

Oliver D, He DZ, Klocker N, Ludwig J, Schulte U, Waldegger S, Ruppersberg JP, Dallos P & Fakler B (2001). Intracellular anions as the voltage sensor of prestin, the outer hair cell motor protein. *Science* **292**, 2340–2343.

Petrovic S, Barone S, Xu J, Conforti L, Ma L, Kujala M, Kere J & Soleimani M (2004). SLC26A7: a basolateral Cl^-/HCO_3^- exchanger specific to intercalated cells of the outer medullary collecting duct. *Am J Physiol Renal Physiol* **286**, F161–F169.

Roos A & Boron WF (1981) Intracellular pH. *Physiol Rev* **61**, 297–434.

Rybalchenko V & Santos-Sacchi J (2008). Anion control of voltage sensing by the motor protein prestin in outer hair cells. *Biophys J* **95**, 4439–4447.

Santos-Sacchi J, Song L, Zheng J & Nuttall AL(2006) Control of mammalian cochlear amplification by chloride anions. *J Neurosci* **26**, 3992–3998.

Schaechinger TJ, Gorbunov D, Halaszovich CR, Moser T, Kugler S, Fakler B & Oliver D (2011). A synthetic prestin reveals protein domains and molecular operation of outer hair cell piezoelectricity. *EMBO J* **30**, 2793–2804.

Schaechinger TJ & Oliver D (2007). Nonmammalian orthologs of prestin (SLC26A5) are electrogenic divalent/chloride anion exchangers. *Proc Natl Acad Sci U S A* **104**, 7693–7698.

Schanzler M & Fahlke C (2012). Anion transport by the cochlear motor protein prestin. *J Physiol* **590**, 259–272.

Shcheynikov N, Wang Y, Park M, Ko SB, Dorwart M, Naruse S, Thomas PJ & Muallem S (2006). Coupling modes and stoichiometry of Cl^-/HCO_3^- exchange by slc26a3 and slc26a6. *J Gen Physiol* **127**, 511–524.

Szatkowski MS & Thomas RC (1986). New method for calculating pHi from accurately measured changes in pHi induced by a weak acid and base. *Pflugers Arch* **407**, 59–63.

Tang J, Pecka JL, Tan X, Beisel KW & He DZ (2011). Engineered pendrin protein, an anion transporter and molecular motor. *J Biol Chem* **286**, 31014–31021.

Tunstall MJ, Gale JE & Ashmore JF (1995). Action of salicylate on membrane capacitance of outer hair cells from the guinea-pig cochlea. *J Physiol* **485**, 739–752.

Wangemann P (2006). Supporting sensory transduction: cochlear fluid homeostasis and the endocochlear potential. *J Physiol* **576**, 11–21.

Wurch T, Lestienne F & Pauwels P (1998). A modified overlap extension PCR method to create chimeric genes in the absence of restriction enzymes. *Biotechnol Tech* **12**, 653–657.

Zheng J, Shen W, He DZ, Long KB, Madison LD & Dallos P (2000). Prestin is the motor protein of cochlear outer hair cells. *Nature* **405**, 149–155.

Author contributions

This work was carried out at the UCL Ear Institute. P.M., N.D. and J.F.A. conceived and designed the experiments; P.M., J.F.A. and K.M. collected and analysed the data, and the article was written by P.M. and J.F.A. All authors approved the final version of the manuscript.

Acknowledgements

This research was supported by European Commission FP6 Integrated Project EUROHEAR, LSHG-CT-20054-512063. We thank J. Mikiel-Hunter for help with some of the early outer hair cell experiments, and B. Fakler, J. Henley and G. Miesenbock for gifts of plasmids.

Author's present address

P. Mistrik: MED-EL, Fuerstenweg 77a, 6020 Innsbruck, Austria.